

The object of this study is a medium-carbon gear steel commonly used for sprockets and gears in mechanical drive systems. The problem to be solved in this study is the limited understanding of the integrated effect of austenitizing temperature, sprocket rotation speed, and quenching medium on surface hardness and microstructural evolution, that makes parameter selection of flame hardening in industry does not optimum. The experiments were conducted by heating the medium-carbon gear steel into austenitizing temperatures of 850°C and 900°C, rotation speeds of 1503 rpm and 1977 rpm, and using water and oil as quenching medium. Specimens were evaluated by using Rockwell hardness tester (B scale) and optical microscopy. The result of this study reveals that the highest surface hardness of 120.08 HRB is achieved at austenitizing temperature of 900°C, rotation speed of 1503 rpm, and quenched by using water. This is also supported by the result of microstructural observations which show very fine martensite. The surface hardening is most affected by quenching medium, while rotation speed has no significant effect on the hardness enhancement. At austenitizing temperature of 900°C, the steel has been in austenite phase, so the increasing rotation speed reduces hardness due to excessive heat input and austenite grain coarsening. The distinctive feature of these results lies in the identification of interaction mechanisms between thermal exposure time and cooling rate. The findings can be practically applied to medium-carbon gear steel components subjected to controlled flame hardening with continuous rotation at speeds of 1503–1977 rpm, followed by water or oil quenching, particularly in small- and medium-scale industrial heat treatment of gears and sprockets

**Keywords:** flame hardening, medium-carbon gear steel, microstructure, quenching medium, surface hardness

# IDENTIFICATION OF THE EFFECT AND MECHANISM OF AUSTENITIZING TEMPERATURE, SPROCKET ROTATION SPEED, AND QUENCHING MEDIUM ON MICROSTRUCTURE AND HARDNESS OF FLAME-HARDENED GEAR STEEL

**Agus Suprpto**

*Corresponding author*

Professor, Engineer, Master of Science, Philosophy Doctor (PhD),  
Intermediate Professional Engineer\*

E-mail: agus.suprpto@unmer.ac.id

ORCID: <https://orcid.org/0009-0007-5973-0381>

**Jumiadi**

Master, Lecturer\*

ORCID: <https://orcid.org/0000-0003-1889-763X>

**Pungky Eka Setyawan**

Master\*

ORCID: <https://orcid.org/0000-0003-0207-3003>

**Mesti Nadya**

Master\*

ORCID: <https://orcid.org/0009-0000-8301-0746>

**Sergius Sadu**

Bachelor\*

ORCID: <https://orcid.org/0009-0008-4156-7368>

\*Department of Mechanical Engineering

Universitas Merdeka Malang

Terusan Raya Dieng str., 62-64, Malang, Indonesia, 65146

Received 05.12.2025

Received in revised form 23.01.2026

Accepted 16.02.2026

Published 26.02.2026

**How to Cite:** Suprpto, A., Jumiadi, P., Setyawan, E., Nadya, M., Sadu, S. (2026). Identification of the effect and mechanism of austenitizing temperature, sprocket rotation speed, and quenching medium on microstructure and hardness of flame-hardened gear steel. *Eastern-European Journal of Enterprise Technologies*, 1 (12 (139)), 25–34. <https://doi.org/10.15587/1729-4061.2026.349675>

## 1. Introduction

Medium carbon steel is a carbon steel that contains 0.3–0.6% carbon and is widely used for power transmission components such as gears, crankshafts, and sprockets [1]. This is due to its excellent combination of strength, toughness, and hardenability, which makes medium carbon steel suitable for active mechanical components, for instance sprocket [2]. Sprocket is used in power transmission systems with high-speed ratios, therefore surface heat treatment is required to provide sufficient toughness to withstand the vibration and adequate wear resistance [3]. Surface hardening

is heat treatment process that object to enhance the surface of specimen but maintain the core toughness [4]. One of surface hardening methods that can be applied to sprocket is flame hardening [5].

Flame hardening is one of phase transformation process that thermally induced in which rapid localized heating causes austenitization of the surface layer, followed by quenching-induced transformation to martensite or mixed transformation products [5, 6]. The resulting hardness and wear resistance are primarily determined by austenite grain size, carbon distribution, cooling rate, and the stability of retained phases [2, 7]. In modern industrial conditions, flame hard-

ening remains attractive due to its ability to implement steep thermal gradients and non-equilibrium cooling paths, which are highly relevant for tailoring surface microstructures.

Despite its widespread application, the fundamental relationships between flame hardening parameters and microstructural evolution are not yet fully understood [6]. Austenitizing temperature directly influences phase homogeneity and austenite grain growth, while component rotation speed affects heat input, thermal exposure time, and temperature uniformity along the treated surface [2, 8]. The choice of quenching medium determines cooling kinetics, which in turn control martensitic transformation, carbide refinement, and the suppression of diffusional transformation products [9, 10]. Existing literature largely examines these parameters independently, leaving a gap in understanding their coupled effects on phase transformation behavior and resultant hardness.

Elaborating the integrated effects of austenitizing temperature, rotation speed, and quenching medium is essential for establishing robust process microstructure property correlations in flame-hardened gear steels [3]. Such knowledge can contribute to the rational design of thermal cycles that promote refined martensitic structures while minimizing grain coarsening and undesirable phase formation. Based on a practical standpoint, these insights can support the optimization of industrial flame hardening practices, improve reproducibility of surface properties, and enhance the overall performance of gear components. Therefore, research devoted to the systematic investigation of microstructural evolution and surface hardness as influenced by flame hardening parameters is scientifically and technologically relevant under modern materials engineering conditions.

---

## 2. Literature review and problem statement

---

Flame hardening is widely applied as a surface heat treatment method to improve hardness and wear resistance through localized austenitization followed by rapid cooling. The work in [5] investigated the influence of flame temperature, torch cap configuration, and quenching period on low-carbon steel. It was shown that flame temperature had the most significant effect on hardness enhancement. However, the study focused on low-carbon steel and evaluated the parameters independently, without analyzing the interaction between thermal exposure and cooling rate. This limitation may be associated with the experimental complexity of controlling multiple coupled parameters during dynamic flame heating.

A subsequent study in paper [6] employed a design of experiments approach to analyze flame temperature, torch distance, and quenching method. The findings identified temperature and quenching medium as dominant factors influencing surface hardness. Nevertheless, the investigation did not extend to phase transformation behavior or microstructural evolution under varying thermal exposure durations. The absence of integrated microstructural analysis may be attributed to the additional metallographic characterization required, which increases experimental cost and analytical effort.

The effect of quenching media on mechanical properties was further examined in paper [9], where different cooling agents altered the yield strength and ductility of mild steel. However, the study emphasized bulk mechanical properties rather than localized surface-hardened layers produced by

flame treatment. Thus, the specific influence of quenching medium on phase transformation in flame-hardened surface regions remained insufficiently addressed.

A similar investigation was reported in [11], where plasma hardening was applied to AISI 420 steel. The results demonstrated that quenching medium strongly influenced martensite formation. Despite these findings, the combined interaction between heating parameters and cooling conditions under rotational heating was not evaluated. This omission may stem from the difficulty of synchronizing heat input, rotational motion, and cooling rate within a single experimental framework.

The influence of rotational speed as a parameter to control heat input was examined in studies [12, 13]. Both studies showed that increasing rotation speed promoted microstructural refinement, particularly grain size reduction. While these findings highlight the role of thermal exposure time, they did not systematically correlate rotation speed with austenitizing temperature and cooling media in an integrated design. The gap may be attributed to the technical challenges associated with transient heat transfer control during continuous rotation flame hardening.

The role of austenitizing temperature in phase formation was discussed in [14], where decreasing temperature from 900°C to 860°C refined prior austenite grain size. Although higher austenitizing temperatures generally enhance carbon dissolution and potential hardness, the interaction between elevated austenitizing temperature and specific quenching media during flame hardening was not examined. As a result, the transformation kinetics under combined thermal and cooling conditions remained insufficiently explored.

Recent findings in paper [15] confirmed that water quenching produces higher cooling rates and refined martensitic structures, whereas oil quenching results in mixed bainite-martensite microstructures. However, these studies did not integrate controlled rotation speed with defined thermal exposure in gear steel applications.

Thus, although temperature, cooling medium, and rotation speed have individually been identified as influential parameters, their combined effect on phase transformation behavior and hardness evolution during flame hardening has not been comprehensively analyzed. The primary challenge lies in achieving controlled and reproducible coupling between thermal exposure, rotational motion, and cooling conditions.

All these considerations allow to assert that it is expedient to conduct a systematic study on the combined influence of austenitizing temperature, rotation speed, and quenching medium on microstructural evolution and surface hardness of medium-carbon gear steel under controlled flame hardening conditions.

---

## 3. The aim and objectives of the study

---

The aim of the study is to identify the effects of combined parameters of flame hardening (austenitizing temperature, sprocket rotation speed, and quenching medium) on the microstructure and surface hardness of flame-hardened gear steel. The findings can be practically applied to medium-carbon gear steel components subjected to controlled flame hardening with continuous rotation at speeds of 1,503–1,977 rpm, followed by water or oil quenching. The optimized parameter combination contributes to improved surface hardness

consistency and enhanced wear resistance, particularly in small- and medium-scale industrial heat treatment of gears and sprockets.

To achieve this aim, the following objectives were accomplished:

- to determine the variation of surface hardness under different combinations of austenitizing temperature, rotation speed, and quenching medium;

- to analyze the microstructural changes and phase transformation behavior resulting from the combined influence of thermal exposure and cooling conditions;

- to identify the dominant mechanisms responsible for hardness enhancement or reduction during flame hardening;

- to establish optimum flame hardening conditions for achieving maximum surface hardness with refined microstructure.

## 4. Materials and methods

### 4.1. The object of the study, hypothesis, and methodological framework

The object of this study is a medium-carbon gear steel commonly used for sprockets and gears in mechanical drive systems [15]. The material used in this study was medium-carbon gear steel equivalent to AISI 1045, commonly applied in gear and sprocket manufacturing. The steel contained approximately 0.42–0.50 wt.% C, 0.60–0.90 wt.% Mn, with trace amounts of Si, P, and S. Prior to flame hardening, the material exhibited a ferrite–pearlite microstructure with an average hardness of 85–88 HRB. The study focuses on the surface layer of the steel subjected to flame hardening, where phase transformations induced by rapid thermal cycles determine the resulting hardness and microstructural state.

The main research hypothesis is that the surface microstructure and hardness of flame-hardened gear steel are not controlled by individual processing parameters alone, but by the combined interaction of austenitizing temperature, rotationally induced thermal exposure, and quenching severity. It is assumed that variations in rotation speed primarily affect heat input and exposure time during austenitization, while the quenching medium determines cooling kinetics and transformation pathways.

Several assumptions and simplifications were adopted in this work. The chemical composition of the gear steel was considered uniform and representative of industrial materials. Heat losses due to convection and radiation were assumed to be consistent across all experiments. The flame characteristics, such as fuel composition and flame geometry, were maintained constant and were not treated as independent variables. Additionally, the analysis was limited to surface hardness and qualitative microstructural features, without considering residual stresses or distortion effects. Fig. 1 illustrates the experimental methodology employed in this study.

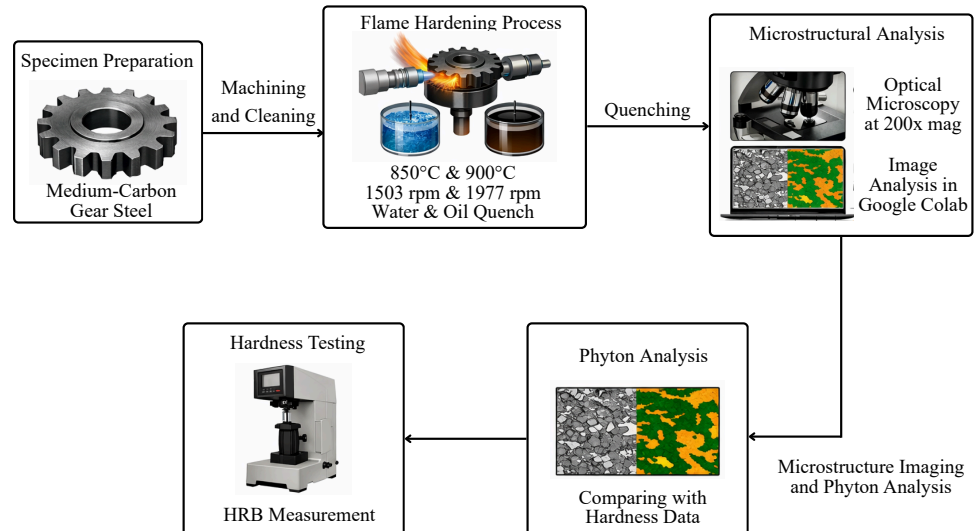


Fig. 1. Experimental methodology flowchart

Fig. 1 presents a schematic overview of the experimental methodology adopted in this study. The workflow begins with specimen preparation of medium-carbon gear steel, followed by flame hardening under controlled austenitizing temperatures and rotation speeds with different quenching media. Subsequently, surface hardness is evaluated using the Rockwell B method, while microstructural characterization is conducted through optical microscopy and Python-based image analysis in Google Colab to support phase identification and quantification.

### 4.2. Material and specimen preparation

The material investigated was a medium-carbon gear steel widely employed in industrial sprocket and gear applications [3]. Specimens were machined into sprocket geometries representative of practical components to ensure realistic thermal boundary conditions during flame hardening, as shown in Fig. 2. Prior to heat treatment, all specimen surfaces were mechanically cleaned and degreased to minimize oxidation and ensure uniform heat absorption.

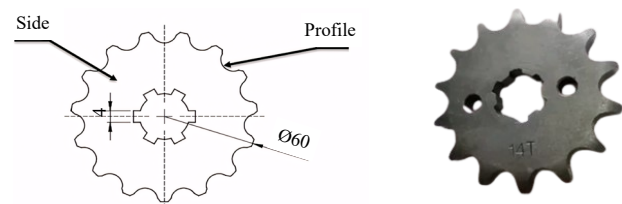


Fig. 2. Geometry and dimensions of specimen

Fig. 2 illustrates the geometry and principal dimensions of the sprocket specimen used in the experimental investigation. The specimen was designed to represent an industrial gear component, ensuring that the geometric features and dimensional characteristics provide realistic thermal boundary conditions during flame hardening. The combination of a schematic drawing and an actual photograph highlights the overall profile, tooth geometry, and key dimensions of the specimen employed throughout the experimental procedures.

### 4.3. Flame hardening procedure

Flame hardening was performed using a controlled flame heating system suitable for surface treatment of rotating

components [16, 17]. Austenitizing temperatures were set at 850°C and 900°C, corresponding to typical industrial practice for medium-carbon steels [18]. During heating, the sprocket specimens were rotated at constant speeds of 1503 rpm and 1977 rpm to control thermal exposure time and heat distribution. Rotation speed in rotary flame hardening controls surface heat exposure, thermal penetration, and microstructural uniformity. The selected speeds of 1503 rpm and 1977 rpm represent moderate and high exposure rates commonly used in industrial practice. A range of 1500–2000 rpm is widely applied for small- to medium-diameter cylindrical components, providing balanced thermal uniformity, controlled heat input, and stable processing conditions. Immediately after reaching the target temperature, the specimens were quenched using either water or oil as the cooling medium. These quenching media were selected to provide different cooling severities. All other processing parameters were maintained constant to isolate the effects of temperature, rotation speed, and quenching condition.

#### 4. 4. Hardness measurement

Surface hardness was measured using the Rockwell B (HRB) method in accordance with standard testing procedures which is ASTM E18 [19]. Hardness testing was performed using a Rockwell hardness tester (Tinius Olsen) with load capacities ranging from 10 to 150 kgf. The HRB scale was selected, as flame hardening is a surface hardening process that produces a hardened layer over a relatively softer core, making the B scale more appropriate for evaluating surface-modified medium-carbon steels without excessive indentation depth. In contrast, the HRC scale is generally applied to fully hardened materials with uniformly high hardness throughout the cross-section. All measurements were conducted in accordance with standard Rockwell testing procedures. The measurements were conducted under appropriate Rockwell scale conditions in accordance with standard testing procedures. Multiple indentations were performed on each specimen at different surface locations to reduce local variability and improve statistical reliability.

#### 4. 5. Microstructural characterization and image analysis using Python

Microstructural characterization was conducted using optical microscopy. Specimens were sectioned perpendicular to the hardened surface, mounted, ground, polished, and etched following standard metallographic procedures to reveal phase constituents. Microstructural observations were conducted using a metallurgical optical microscope (Nikon Eclipse MA100) at 200× magnification after standard metallographic preparation and Nital etching. In addition to qualitative optical examination, quantitative microstructural analysis was performed using Python-based image processing implemented in the Google Colab environment, employing OpenCV and NumPy libraries for grayscale conversion, threshold segmentation, and quantitative phase analysis [20, 21]. Digital micrographs were uploaded to the Colab platform and processed using open-source Python libraries for scientific computing and image analysis. The workflow included grayscale conversion, noise reduction, contrast enhancement, image segmentation, and threshold-based phase differentiation to distinguish microstructural constituents such as martensite and bainite based on grayscale intensity and morphological features.

This computational approach was employed to support objective and reproducible microstructural assessment by reducing operator bias inherent in manual interpretation. The same image processing parameters were applied consistently across all samples to ensure comparability of the analyzed microstructures.

## 5. Results of flame hardening on medium-carbon gear steel

### 5. 1. Surface hardness response under different flame hardening conditions

The effect of austenitizing temperature, sprocket rotation speed, and quenching medium on the surface hardness of medium-carbon gear steel was evaluated through systematic flame hardening experiments. The average surface hardness values obtained under different processing conditions are summarized in Table 1.

Table 1

Surface hardness of flame-hardened gear

Temperature (°C)	Speed (rpm)	Quench	Hardness ( $HR_B$ )
Base metal			105.50
850	1503	Water	117.17
850	1503	Oil	110.50
850	1977	Water	117.58
850	1977	Oil	109.75
900	1503	Water	120.08
900	1503	Oil	108.83
900	1977	Water	113.33
900	1977	Oil	106.50

Table 1 presents the surface hardness values of the gear steel before and after flame hardening. The base metal exhibits a surface hardness of 105.50 HRB. Following flame hardening, the surface hardness increases to values ranging from 106.50 to 120.08 HRB, depending on the applied processing parameters.

As shown in Table 1, the base metal exhibits a surface hardness of 105.50 HRB. After flame hardening, the hardness values increase to a range between 106.50 and 120.08 HRB, depending on the applied processing parameters. For specimens treated at an austenitizing temperature of 850°C, water quenching produces higher hardness values, ranging from 117.17 to 117.58 HRB, compared with oil quenching, which results in hardness values between 109.75 and 110.50 HRB. A similar trend is observed at an austenitizing temperature of 900°C, where the highest hardness value of 120.08 HRB is achieved at a rotation speed of 1503 rpm with water quenching. Oil-quenched specimens at 900°C show comparatively lower hardness values, ranging from 106.50 to 108.83 HRB.

### 5. 2. Microstructural evolution of medium-carbon gear steel after flame hardening

The microstructural observations presented in Fig. 3 are intended to complement the surface hardness data by providing a visual description of the phase constituents formed under different flame hardening conditions.

Fig. 3 presents the optical microstructures of the medium-carbon gear steel flame hardened at an austenitizing

temperature of 850°C under different rotation speeds and quenching media. The micrographs correspond to:

- Fig. 3, *a* - 1503 rpm with water quenching;
- Fig. 3, *b* - 1503 rpm with oil quenching;
- Fig. 3, *c* - 1977 rpm with water quenching;
- Fig. 3, *d* - 1977 rpm with oil quenching.

For specimens quenched in water, as shown in Fig. 3, *a*, *c*, the microstructures are dominated by very fine martensitic features distributed uniformly across the observed surface region. In contrast, specimens quenched in oil, shown in Fig. 3, *b*, *d*, exhibit microstructures consisting of martensite accompanied by regions of lower bainite. While Fig. 4 presents the optical microstructures of the medium-carbon gear steel flame hardened at an austenitizing temperature of 900°C under different rotation speeds and quenching media.

Fig. 4 presents the optical microstructures of the medium-carbon gear steel flame hardened at an austenitizing temperature of 900°C under different combinations of rotation speed and quenching medium. The micrographs correspond to:

- a*) 1503 rpm with water quenching;
- b*) 1503 rpm with oil quenching;
- c*) 1977 rpm with water quenching;
- d*) 1977 rpm with oil quenching.

The microstructure in Fig. 4, *a* is characterized by very fine martensite distributed uniformly across the observed region. Fig. 4, *b* presents a microstructure consisting of martensite with the presence of lower bainite. At a higher rotation speed, the specimen quenched in water, shown in Fig. 4, *c*, exhibits a fine martensitic microstructure. In contrast, the specimen quenched in oil at 1977 rpm, presented in Fig. 4, *d*, presents a microstructure composed of martensite accompanied by upper bainite.

Python-based image analysis was employed to complement the optical microstructural observations by quantitatively estimating the phase constituents formed under different flame hardening conditions. The following Fig. 5 presents the corresponding phase estimation results.

As shown in Fig. 5, the results of automatic phase classification into three distinct phases based on microstructural intensity and texture. The spatial distribution of colors indicates the presence of homogeneous microstructural zones, transition regions, and areas with high feature density associated with intensive plastic deformation. Based on the Python-based analysis, the estimated phase constituents formed under each treatment condition are summarized at Table 2.

Table 2 indicates that, at 850°C, the phase distributions are relatively comparable across different rotation speeds, with only minor variations between water- and oil-quenched specimens. Similarly, Fig. 6 presents the automatic phase classification results for specimens austenitized at 900°C.

Table 2

Estimated phase distribution of medium-carbon gear steel flame hardened at an austenitizing temperature of 850°C obtained using Python-based image analysis

Specimen	Rotation speed (rpm)	Quenching medium	Martensite (Fine / very fine) (%)	Bainite (lower / upper) (%)	Martensite (coarser / transitional) (%)
<i>a</i>	1503	Water	33.65	32.71	33.64
<i>b</i>	1503	Oil	33.64	33.02	33.34
<i>c</i>	1977	Water	33.04	33.05	33.91
<i>d</i>	1977	Oil	32.91	33.24	33.85

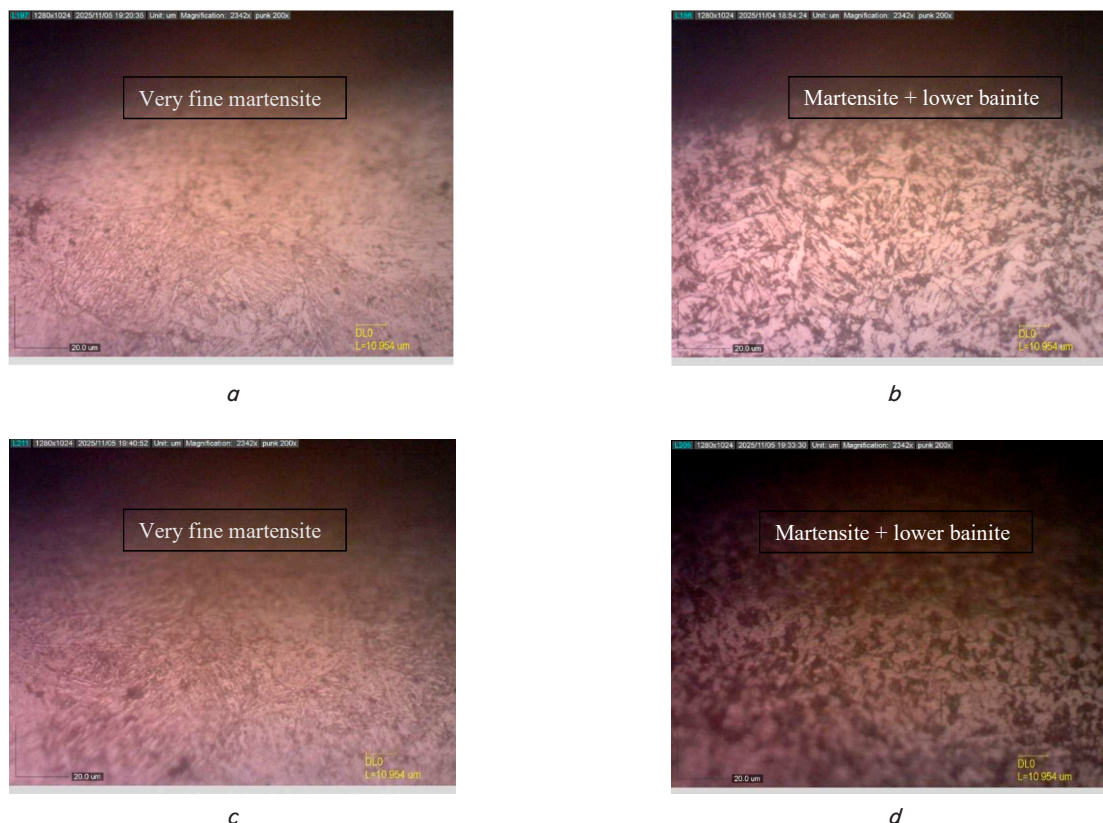


Fig. 3. Microstructure of medium carbon gear steel at austenitizing temperature of 850°C: *a* – sprocket rotation of 1503 rpm with water quenching; *b* – sprocket rotation of 1503 rpm with oil quenching; *c* – sprocket rotation of 1977 rpm with water quenching; *d* – sprocket rotation of 1977 rpm with oil quenching

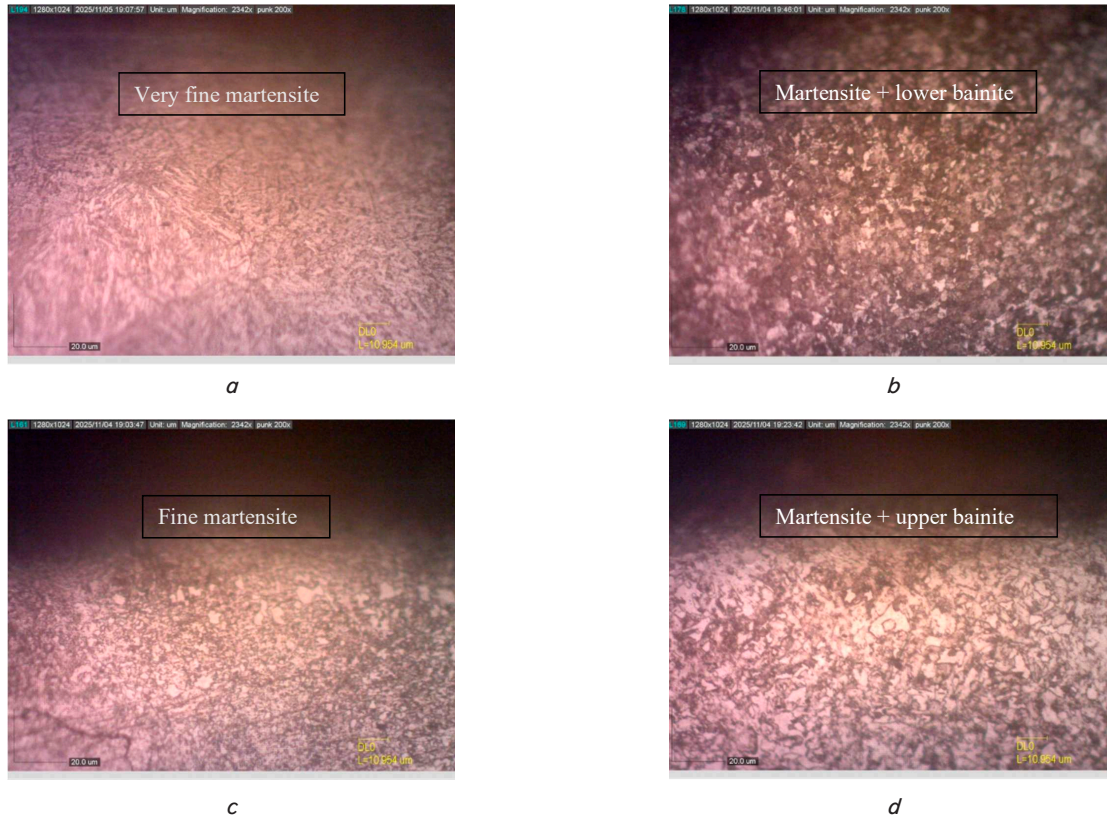


Fig. 4. Microstructure of medium carbon gear steel at austenitizing temperature of 900°C: *a* – sprocket rotation of 1503 rpm with water quenching; *b* – sprocket rotation of 1503 rpm with oil quenching; *c* – sprocket rotation of 1977 rpm with water quenching; *d* – sprocket rotation of 1977 rpm with oil quenching

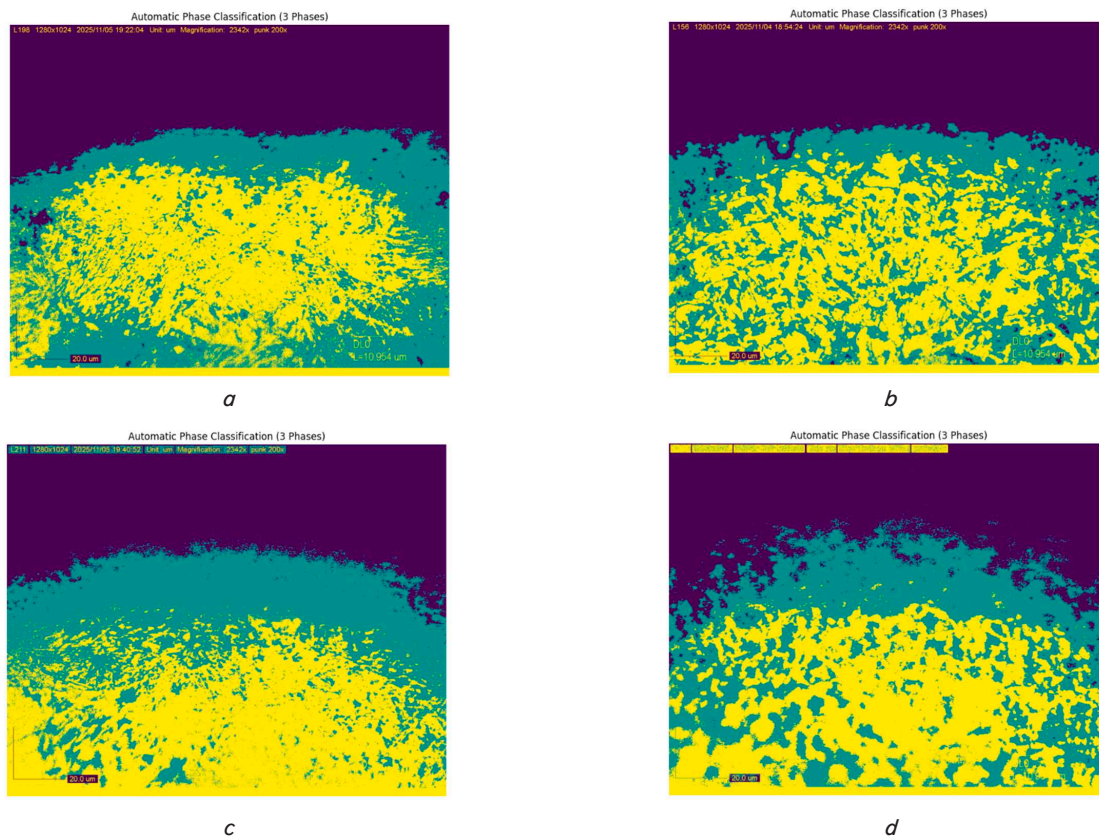


Fig. 5. Automatic phase classification of the microstructure at an austenitizing temperature of 850°C, obtained using Python-based image analysis in Google Colab: *a* – sprocket rotation of 1503 rpm with water quenching; *b* – sprocket rotation of 1503 rpm with oil quenching; *c* – sprocket rotation of 1977 rpm with water quenching; *d* – sprocket rotation of 1977 rpm with oil quenching

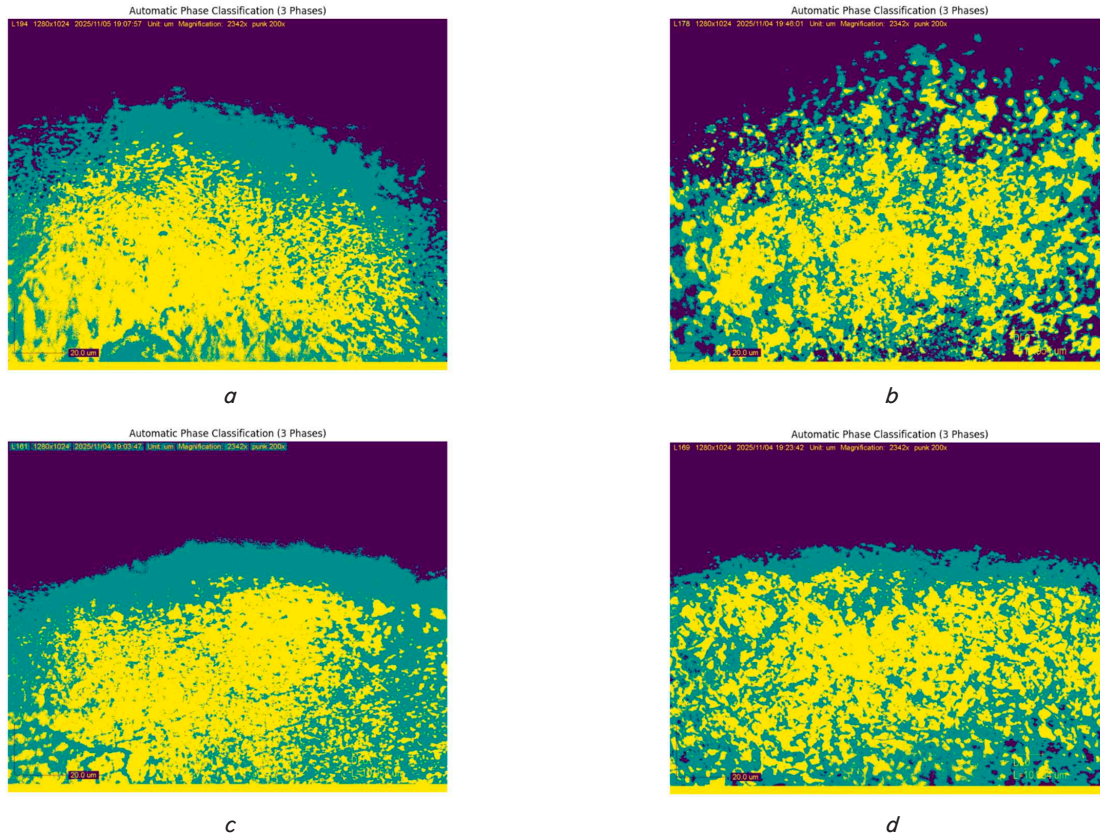


Fig. 6. Automatic phase classification of the microstructure at an austenitizing temperature of 900°C, obtained using Python-based image analysis in Google Colab: *a* – sprocket rotation of 1503 rpm with water quenching; *b* – sprocket rotation of 1503 rpm with oil quenching; *c* – sprocket rotation of 1977 rpm with water quenching; *d* – sprocket rotation of 1977 rpm with oil quenching

A similar phase estimation was conducted for specimens austenitized at 900°C as shown in Fig. 6, and the results are summarized in Table 3.

Table 3

Estimated phase distribution of medium-carbon gear steel flame hardened at an austenitizing temperature of 900°C obtained using Python-based image analysis

Specimen	Rotation speed (rpm)	Quenching medium	Martensite (fine / very fine) (%)	Bainite (lower / upper) (%)	Martensite (coarser / transitional) (%)
(a)	1503	Water	33.20	32.92	33.89
(b)	1503	Oil	32.80	33.29	33.91
(c)	1977	Water	33.14	33.09	33.77
(d)	1977	Oil	33.63	33.04	33.33

The corresponding phase fractions are summarized in Table 3. Compared with the 850°C condition, the results at 900°C indicate a redistribution of martensitic and bainitic morphologies, particularly at higher rotation speed and under oil quenching. These trends suggest that increased thermal exposure prior to quenching alters phase transformation behavior. Overall, the combined optical and computational analyses demonstrate a clear relationship between processing parameters, microstructural evolution, and surface hardness, providing a coherent interpretation of the flame hardening response of medium-carbon gear steel.

### 5.3. Dominant mechanisms responsible for hardness enhancement during flame hardening

The dominant mechanism that is responsible for surface hardness enhancement on medium-carbon gear steel is due to microstructural phase formation that is influenced by flame temperature and quenching medium. Table 4 shows the hardness test result and microstructural of medium-carbon gear steel with several variations.

Table 4

Comparison of hardness test results and microstructural phase of medium-carbon gear steel

Specimen	Temperature (°C)	Speed (rpm)	Quenching medium	Dominant micro-structure	Hardness (HR <sub>B</sub> )
1	850	1503	Water	Very fine martensite	117.17
2	850	1503	Oil	Martensite + lower bainite	110.50
3	850	1977	Water	Very fine martensite	117.58
4	850	1977	Oil	Martensite + lower bainite	109.75
5	900	1503	Water	Very fine martensite	120.08
6	900	1503	Oil	Martensite + lower bainite	108.83
7	900	1977	Water	fine martensite	113.33
8	900	1977	Oil	Martensite + upper bainite	106.50

Table 4 shows the comparison result of hardness test and microstructural phase formation of medium-carbon gear steel.

Based on this table, it can be observed that the dominant mechanism influencing the increase or decrease in surface hardness is grain refinement, which is primarily governed by the austenitizing temperature and the cooling rate. The results further indicate that specimen 5, processed at an austenitizing temperature of 900°C, a rotation speed of 1503 rpm, and water as the quenching medium, exhibited a very fine martensitic phase and achieved the highest hardness value.

#### 5.4. Optimized flame hardening conditions for maximum surface performance

Table 5 presents the optimum flame hardening parameters that resulted in the highest hardness value and the corresponding microstructural phases formed.

Based on Table 5, it can be concluded that the optimum parameters for enhancing the surface hardness of medium-carbon steel are an austenitizing temperature of 900°C, a rotation speed of 1503 rpm, and water as the quenching medium. This condition significantly influences the surface hardening mechanisms of medium-carbon gear steel.

Table 5

Optimum parameter for maximum surface medium-carbon gear steel performance

Temperature (°C)	Speed (rpm)	Quenching medium	Dominant micro-structure	Hardness (HR <sub>B</sub> )
900	1503	Water	Very fine martensite	120.08

## 6. Discussion of the results of flame hardening effect on the properties of medium-carbon steel

The experimental results demonstrate that the surface hardness and microstructural evolution of flame-hardened medium-carbon gear steel are determined by the combined effects of austenitizing temperature, sprocket rotation speed, and quenching medium. As summarized in Table 1, all flame-hardened specimens exhibit significantly higher surface hardness than the base metal, confirming that surface phase transformation was successfully achieved under all investigated conditions [22]. Among the processing variables, the quenching medium exerts the most pronounced influence on surface hardness [3, 9]. Water-quenched specimens consistently show higher hardness values than oil-quenched specimens, reflecting the higher cooling severity of water, which effectively suppresses diffusion-controlled transformations and promotes a predominantly martensitic transformation during quenching, in agreement with widely reported behavior for medium-carbon steels [23, 24].

At an austenitizing temperature of 850°C, the effect of sprocket rotation speed on surface hardness is minimal. Water-quenched specimens exhibit nearly identical hardness values at both investigated rotation speeds, indicating that the thermal input at this temperature is sufficient to achieve uniform austenitization without inducing significant austenite grain growth [13]. In contrast, oil-quenched specimens treated at the same temperature show lower hardness, which correlates with the formation of mixed martensite-bainite microstructures observed in Fig. 3. The presence of bainite, enabled by the lower cooling rate of oil, inherently reduces hardness relative to fully martensitic structures [9, 23, 25].

When the austenitizing temperature is increased to 900°C, the influence of rotation speed becomes more evident. As shown in Table 1, increasing rotation speed leads to a reduction in surface

hardness, particularly under water-quenching conditions. This trend is attributed to prolonged thermal exposure during flame heating [5], which promotes austenite grain coarsening prior to quenching. Coarser prior-austenite grains reduce martensite nucleation density and increase the austenite or bainitic transformation, ultimately resulting in lower hardness [26]. This interpretation is supported by the microstructural observations in Fig. 4, where coarser features are visible at higher rotation speed.

The microstructural observations in Fig. 3, 4 are further corroborated by the Python-based image analysis results presented in Tables 2, 3. Although the estimated phase fractions appear numerically similar across several conditions, the redistribution among martensitic morphological categories and bainitic constituents reveals subtle but meaningful differences in microstructural refinement. At 850°C, phase distribution shows limited sensitivity to rotation speed, confirming that temperature dominates transformation behavior in this regime. At 900°C, however, increased rotation speed results in a measurable shift toward coarser martensitic morphologies and a higher contribution of bainitic constituents, highlighting the role of rotation speed as an effective thermal exposure parameter rather than merely a mechanical variable. The integration of optical microscopy with Python-based phase estimation (Fig. 5, 6) reduces operator subjectivity and provides semi-quantitative validation of visual interpretations, representing a methodological improvement over purely qualitative metallographic analysis [21].

These results demonstrate that hardness evolution during flame hardening cannot be adequately explained by considering austenitizing temperature, rotation speed, or quenching medium in isolation. Instead, the interaction between thermal input, rotational exposure time, and cooling rate determines austenite stability prior to quenching and controls the resulting phase transformation pathways. Within the investigated parameter space, the combination of a 900°C austenitizing temperature, a rotation speed of 1503 rpm, and water quenching represents a functioning balance between sufficient carbon dissolution, controlled thermal exposure that avoids excessive grain coarsening, and rapid cooling that ensures a dominant martensitic transformation. This condition yields the highest surface hardness (120.08 HRB) together with a refined martensitic microstructure, as evidenced in Table 1 and Fig. 3, 4. The results of this study are almost the same as the results of other studies which show that the highest hardness was obtained in specimens with water cooling media, which reached 301 HV with a conversion of 106 HRB [3].

The present findings demonstrate that optimal surface properties arise from a balanced interaction among thermal input, exposure duration, and quenching kinetics [27]. These results are consistent with general trends reported in flame hardening literature, while extending current understanding by explicitly accounting for the coupled influence of rotational motion and thermal history in flame-hardened gear components [5, 16].

Despite these contributions, several limitations of the present study should be acknowledged. The investigation focuses primarily on surface hardness and microstructural characterization, without direct assessment of residual stresses, wear resistance, or fatigue performance, which are critical for gear service applications. In addition, the Python-based image analysis provides relative phase estimation rather than absolute phase quantification, and its accuracy depends on image quality and segmentation parameters. Despite these limitations, the scientific novelty of this study lies in the combined evaluation of rotation speed, quenching medium, and controlled flame heating on the surface hardening behavior of medium-carbon gear

steel. The results clarify the previously unresolved relationship between rotational kinematics during flame hardening and resulting hardness-microstructure gradients, thereby addressing the research gap identified in the literature.

Future work should therefore incorporate mechanical performance testing under simulated service conditions, residual stress measurement, and numerical simulation of transient thermal fields to further elucidate the process-structure-property relationships and enhance the industrial applicability of the proposed flame hardening strategy. Despite these needs for further investigation, the present findings already demonstrate practical relevance. The results are applicable to flame hardening of gears and sprockets used in automotive, agricultural, and industrial machinery, particularly under continuous rotational flame heating with controlled quenching. The expected effects include improved surface hardness uniformity, enhanced wear resistance, and extended service life of gear components.

---

## 7. Conclusion

---

1. The variation of surface hardness under different flame hardening has been identified clearly. There are differences in function about austenitizing temperature, rotation speed of sprocket, and quenching medium on surface hardness that has been measured. According to the measurements, the specimen quenched in water achieved a higher surface hardness of 120.08 HRB, compared to the oil-quenched specimen.

2. The results demonstrate that the combined influence of thermal exposure and cooling conditions significantly affects phase transformation behavior. Water quenching at 900°C and 1503 rpm produced a predominantly martensitic microstructure with the highest hardness of 120.08 HRB, indicating rapid transformation from austenite to martensite. In contrast, oil quenching at 850°C and 1503 rpm resulted in a mixed martensite–bainite structure with a maximum hardness of 110.5 HRB, reflecting slower cooling rates and partial diffusion-controlled transformation. These findings confirm that higher austenitizing temperature coupled with rapid cooling promotes more complete martensitic transformation and greater hardness enhancement.

3. The dominant mechanism that responsible for the surface hardness enhancement or reduction during flame hardening is the combined effect of increased austenitizing temperature and higher cooling rate. Increasing the austenitizing temperature from 850°C to 900°C, coupled with water quenching at 1503 rpm, resulted in the highest hardness of 120.08 HRB, compared to 110.5 HRB obtained under oil quenching at 850°C and 1503 rpm. This improvement is associated with enhanced carbide dissolution and carbon enrichment of austenite, promoting more complete martensitic transformation. Even though the excessive temperature with prolonged thermal exposure may reduce the hardness. Rotation speed significantly affects the thermal input and austenitizing uniformity, where at the lower

speeds (1503 rpm) allowing more complete martensitic transformation and higher surface hardness.

4. The optimum flame hardening condition for achieving maximum surface hardness and fine microstructure can be identified in the combination of austenitizing temperature at 900°C, rotation speed of sprocket at 1503 rpm, and water quenching. These combination parameters achieve the highest surface hardness that accompanied by fine martensitic microstructure.

---

## Conflict of interest

---

The authors declare that they have no conflict of interest in relation to this study, whether financial, personal, authorship or otherwise, that could affect the study and its results presented in this paper.

---

## Financing

---

The study was performed without financial support.

---

## Data availability

---

Manuscript has no associated data.

---

## Use of artificial intelligence

---

The authors declare the use of generative AI in the research and writing process. According to the GAIDeT taxonomy (2025), the following tasks were delegated to GAI tools under full human supervision:

- creation of algorithms for data analysis;
- proofreading and editing;
- translation.

The GAI tool used was: ChatGPT-5.2, Google Colab, and Google Translate.

Responsibility for the final manuscript lies entirely with the authors.

GAI tools are not listed as authors and do not bear responsibility for the final outcomes.

---

## Authors' contributions

---

**Agus Suprpto:** Conceptualization, Supervision, Writing – original draft; **Jumiadi Jumiadi:** Methodology, Investigation, Resource; **Pungky Eka Setyawan:** Formal analysis, Data curation, Visualization; **Mesti Nadya:** Software, Formal analysis, Writing – review & editing; **Sergius Sadu:** Methodology, Investigation, Resource.

---

## References

1. Haiko, O., Pallaspuuro, S., Javaheri, V., Kaikkonen, P., Ghosh, S., Valtonen, K., Kaijalainen, A., Kömi, J. (2023). High-stress abrasive wear performance of medium-carbon direct-quenched and partitioned, carbide-free bainitic, and martensitic steels. *Wear*, 526-527, 204925. <https://doi.org/10.1016/j.wear.2023.204925>
2. Yu, Q., Zhao, Y., Zhao, F. (2025). Effect of austenitizing temperature on microstructure and mechanical properties of medium carbon spring steel. *Materials Letters: X*, 26, 100251. <https://doi.org/10.1016/j.mlblux.2025.100251>
3. Fattah, R. N., Sugiyanto, S., Priyambodo, B. H., Nurhidayat, A., Yaqin, R. I. (2023). Rekayasa Peningkatan Kekerasan Permukaan Gear Sprocket Sepeda Motor dengan Metode Quenching Variasi Media Pendingin. *Quantum Teknika: Jurnal Teknik Mesin Terapan*, 5 (1), 8–13. <https://doi.org/10.18196/jqt.v5i1.19418>

4. Gathmann, M., Tönnißen, N., Baron, C., Kostka, A., Steinbacher, M., Springer, H. (2024). Surface hardening of high modulus steels through carburizing and nitriding: First insights into microstructure property relationships. *Surface and Coatings Technology*, 494, 131354. <https://doi.org/10.1016/j.surfcoat.2024.131354>
5. Thamilarasan, J., Karunakaran, N., Nanthakumar, P. (2021). Optimization of oxy-acetylene flame hardening parameters to analysis the surface structure of low carbon steel. *Materials Today: Proceedings*, 46, 4169–4173. <https://doi.org/10.1016/j.matpr.2021.02.680>
6. Jeyaraj, S., Arulshri, K.P., Harshavardhan, K., Sivasakthivel, P.S. (2015). Optimization of Flame Hardening Process Parameters Using L9 Orthogonal Array of Taguchi Approach. *International Journal of Engineering and Applied Sciences*, 2. Available at: <https://www.semanticscholar.org/paper/Optimization-of-Flame-Hardening-Process-Parameters-Jeyaraj-Arulshri/227823755df2ac8da50e005822418fa1e220d864>
7. Zhang, Y., Liu, W., Long, X., Liu, Z., Li, Y., Yang, Z., Zhang, Y. (2025). Combining in-situ technology to study the influence of bainite morphology on the strength and toughness properties of medium-carbon bainitic steel. *Journal of Materials Research and Technology*, 36, 34–44. <https://doi.org/10.1016/j.jmrt.2025.03.106>
8. Luo, R., Chen, J., Ding, H., Zhang, P., Liao, J., Yu, Y. et al. (2025). The effect of quenching cooling rate on the microstructure and tensile/compressive behaviors of 2Cr12Ni martensitic stainless steel. *Journal of Materials Research and Technology*, 36, 2994–3006. <https://doi.org/10.1016/j.jmrt.2025.03.227>
9. Ajoge, E. O., James, M. (2024). Influence of Different Quenching Media on the Mechanical Properties of Mild Steel – A Case Study of Coconut Oil, Mineral Oil, Jatropha Oil, and Water. *Metall Alloy*, 10, 1–8. Available at: <https://journalspub.com/wp-content/uploads/2024/12/1-8Influence-of-Different-Quenching-Media.pdf>
10. Li, B., Bai, W., Yang, K., Hu, C., Wei, G., Liu, J. et al. (2024). Revealing the microstructural evolution and strengthening mechanism of Mg-5.5Gd-3Y-1Zn-0.5Mn alloy in centrifugal casting and subsequent hot rolling. *Journal of Alloys and Compounds*, 984, 173950. <https://doi.org/10.1016/j.jallcom.2024.173950>
11. Kombayev, K., Nedobitkov, A., Gridunov, I., Kozhakhmetov, Y., Khoshnaw, F., Aibar, K. (2025). Surface crack analysis and quality enhancement of 30X13 (AISI 420) martensitic stainless steel gate valve shutters via electrolytic plasma hardening. *Results in Engineering*, 26, 104966. <https://doi.org/10.1016/j.rineng.2025.104966>
12. Oliaei, M., Jamaati, R., Jamshidi Aval, H. (2025). Optimizing microstructure and performance: The impact of pre-deformation and rotational speed on friction stir processed Cu-W composites. *Journal of Advanced Joining Processes*, 11, 100308. <https://doi.org/10.1016/j.jajp.2025.100308>
13. Bararpour, S. M., Jamshidi Aval, H., Jamaati, R., Javidani, M. (2024). Effect of heat treatment before fast multiple rotation rolling on friction surfaced Al–Si–Cu alloy. *Journal of Materials Research and Technology*, 33, 940–953. <https://doi.org/10.1016/j.jmrt.2024.09.119>
14. Kristiadi, S., Lesmanah, U., Raharjo, A. (2023). Pengaruh Variasi Media Pendingin Terhadap Kekerasan dan Mikrostruktur Pada Pengecoran Aluminium 6061. *Ring Mechanical Engineering*, 2(2), 101–112. <https://doi.org/10.33474/rm.v2i2.19906>
15. Li, Q., Li, W., Li, M., Su, M., Hu, Z., Ma, H. et al. (2025). Improving the high stress abrasive wear resistance of medium carbon quenched and partitioned bainitic steel by controlling the phase transformation sequence. *Journal of Materials Research and Technology*, 38, 2808–2819. <https://doi.org/10.1016/j.jmrt.2025.08.109>
16. Li, X., Li, Z., Dong, L., Liu, B., Wang, H., Shi, T. et al. (2025). Study of microstructure evolution and fatigue crack extension properties of 42CrMo steel strengthened by induction hardening. *Journal of Materials Research and Technology*, 35, 3887–3901. <https://doi.org/10.1016/j.jmrt.2025.02.069>
17. Xin, M., Wang, Z., Lu, B., Li, Y. (2022). Effects of different process parameters on microstructure evolution and mechanical properties of 2060 Al–Li alloy during vacuum centrifugal casting. *Journal of Materials Research and Technology*, 21, 54–68. <https://doi.org/10.1016/j.jmrt.2022.08.147>
18. Sundari, E., Taufikurrahman, Fahlevi, R. (2018). Analisa pengaruh pack carburizing terhadap sifat mekanis sprocket imitasi sepeda motor menggunakan arang kayu gelam dan serbuk cangkang remis sebagai katalisator. *Austenit*, 10 (2), 72–78. <https://doi.org/10.5281/ZENODO.4547659>
19. ASTM E18-22. Standard Test Methods for Rockwell Hardness of Metallic Materials. <https://doi.org/10.1520/e0018-22>
20. Ackermann, M., Iren, D., Wesselmecking, S., Shetty, D., Krupp, U. (2022). Automated segmentation of martensite-austenite islands in bainitic steel. *Materials Characterization*, 191, 112091. <https://doi.org/10.1016/j.matchar.2022.112091>
21. Chakraborty, S., Björk, J., Dahlqvist, M., Rosen, J., Heintz, F. (2026). A survey of AI-supported materials informatics. *Computer Science Review*, 59, 100845. <https://doi.org/10.1016/j.cosrev.2025.100845>
22. Ponhan, K., Jiandon, P., Juntaracena, K., Potisawang, C., Kongpuang, M. (2024). Enhanced microstructures, mechanical properties, and machinability of high performance ADC12/SiC composites fabricated through the integration of a master pellet feeding approach and ultrasonication-assisted stir casting. *Results in Engineering*, 24, 102937. <https://doi.org/10.1016/j.rineng.2024.102937>
23. Pizetta Zordão, L. H., Oliveira, V. A., Totten, G. E., Canale, L. C. F. (2019). Quenching power of aqueous salt solution. *International Journal of Heat and Mass Transfer*, 140, 807–818. <https://doi.org/10.1016/j.ijheatmasstransfer.2019.06.036>
24. Moshokoa, N. A., Makhatha, E., Raganya, L., Makoana, N. W., Mkhonto, D., Phasha, M. (2026). Study of phase constituents, microstructural evolution, tensile properties and micro-Vickers hardness of as-cast and water quenched Ti-Mo-Fe alloys. *Results in Materials*, 29, 100885. <https://doi.org/10.1016/j.rinma.2026.100885>
25. dos Santos, S. L., Santos, S. F. (2024). Heat treatment of the SAE 9254 spring steel: Influence of cooling rate on the microstructure and microhardness. *Next Materials*, 3, 100175. <https://doi.org/10.1016/j.nxmte.2024.100175>
26. Arabacı, U. (2024). The effects of oil-quenching and over-tempering heat treatments on the dry sliding wear behaviours of 25CrMo4 steel. *Heliyon*, 10 (3), e25589. <https://doi.org/10.1016/j.heliyon.2024.e25589>
27. Zhang, L., Miao, Y., Wang, J., Zhang, M., Liu, Y., Zhou, Y. et al. (2025). Research on the microstructural differences and mechanical response mechanisms of martensitic stainless steel additive manufacturing under cross-scale heat input control. *Materials & Design*, 260, 115132. <https://doi.org/10.1016/j.matdes.2025.115132>